

On the Infrared $A^2\Pi_i - X^2\Sigma^+$ System of Aluminium Monoxide in Relation with the Spectra of M Giant- and Mira-Type Stars

A. Bernard and R. Gravina

Observatoire de Lyon, Université Claude Bernard (Lyon I), Saint-Genis Laval, France, and
Laboratoire de Spectrométrie Ionique et Moléculaire, Université Claude Bernard (Lyon I),
Villeurbanne, France*

Z. Naturforsch. **39a**, 1049–1055 (1984); received May 16, 1984

From combinations between known ultraviolet transitions of the AlO molecule line positions in the $A^2\Pi_i - X^2\Sigma^+$ system are tentatively proposed. Indeed, the available data on the $C^2\Pi_r \rightarrow X^2\Sigma^+$ and $C^2\Pi_r \rightarrow A^2\Pi_i$ transitions permit us to derive about 2400 energy level differences in the A–X system corresponding to the six v -connected bands 0–0, 0–1, 0–2, 1–0, 1–1 and 1–2. A unique and consistent set of rovibrational constants is derived from a global fitting, allowing to reproduce the observed differences with a total standard deviation of 0.053 cm^{-1} . A catalogue of vacuum line wavenumbers in the six bands is generated and can be made available on request. The synthetic spectra are expected to represent properly the true spectra at least up to $J \sim 35.5$ and can therefore be of usefulness for the detection of the system in the spectra of M giant- and Mira-type stars.

Franck-Condon factors and r-centroids appropriate to RKR potentials and estimates of intensities in emission are given for bands up to $v' = 5$, $v'' = 8$.

More reliable values for the internal partition functions and dissociation constants of AlO are computed for temperatures between 1000 and 8000 K. All the known and predicted electronic states are taken into account, and present or recent values for the molecular parameters and dissociation energy are used.

1. Introduction

The existence of the AlO molecule in cool stellar atmospheres has first been shown through the identification of the blue-green bands of the $B^2\Sigma^+ \rightarrow X^2\Sigma^+$ system in the spectrum of the variable star Mira Ceti [1] and then in the spectra of normal M giant stars of type later than M3 [2]. The behaviour of the strongest band of the system, the 0–0 band with head at 4842 Å , was thoroughly analyzed [3] from a survey of numerous spectrograms. The conclusions were that in the spectra of normal M giant stars the intensities of the absorption bands of AlO are well correlated with the spectral type as defined from the TiO criterion; on the other hand, in Mira-type variable stars the AlO bands can greatly vary from cycle to cycle, being abnormally strong or weak for the spectral type or even at times going over into emission.

Luck and Lambert [4] and Murty [5] have emphasized the need for another electronic transition to be observed in the stellar spectra in order to better

determine the depth of formation of the AlO molecules and the temperature changes occurring within the atmosphere during the times when AlO is observed. Founding upon ab initio calculations of band oscillator strengths [6] and estimated molecular column densities for M-type stars [7], Luck and Lambert suggested that the $A^2\Pi_i \rightarrow X^2\Sigma^+$ system could be detectable; they finally concluded that the simultaneous observations of the blue-green and the infrared $A \rightarrow X$ transitions should provide important information as to the nature of the mechanisms controlling the Mira phenomenon.

Unfortunately, the $A \rightarrow X$ system has not yet been observed in rotation. Knight and Weltner [8] first observed the absorption from the ground state to low vibrational levels of the A state; then the chemiluminescence from the $A \rightarrow X$ transition [9], [10] was investigated but no direct information is available until now as to the expected most intense bands of the system which do appear in the $2\text{ }\mu\text{m}$ region. A first attempt to detect the 1–0 band [4] in high-resolution spectra of Mira-type stars (o Cet, R Leo, W Hya) and M supergiants (W Ori, α Her, α Sco), based on extrapolated constants for the $A^2\Pi_i$ ($v = 1$) level, appeared negative, but the possible uncertainty in the predictions of the line posi-

* 43, Boulevard du 11 Novembre 1918, 69622 Villeurbanne, France.

Reprint requests to Dr. A. Bernard, Observatoire de Lyon, 69230 Saint-Genis Laval, France.



tions was evaluated to 1 cm^{-1} . Molecular constants now exist for the A state ($v = 0, 1$) from the works of McDonald and Innes [11] on the $D^2\Sigma^+ \rightarrow A^2\Pi_i$ ($v = 0$) system and Singh and Saksena [12, 13] on the $E^2\Delta_i \rightarrow A^2\Pi_i$ ($v = 0, 1$) and $C^2\Pi_r \rightarrow A^2\Pi_i$ ($v = 0, 1$) systems respectively, while the constants of the $X^2\Sigma^+$ state are already known very accurately from earlier studies up to $v = 5$.

The aim of this paper is to present a homogeneous set of molecular constants for the X ($v = 0, 1, 2$) and A ($v = 0, 1$) states and propose a catalogue of line wavenumbers. The calculations of the synthetic spectra for the six bands 0–0, 0–1, 0–2, 1–0, 1–1 and 1–2 are based upon combinations of recent accurate measurements of the ultraviolet transitions $C \rightarrow X$ [14] and $C \rightarrow A$ [13]. Using the present constants, Franck-Condon factors and r-centroids are then given together with estimates of the relative intensities in emission for bands up to $v' = 5$, $v'' = 8$. Finally, new estimations of the internal partition functions (since X and A states are the major contributors) and equilibrium dissociation constants are made based on present or recent spectroscopic data (particularly for the dissociation energy of AlO).

2. The $A^2\Pi_i \rightarrow X^2\Sigma^+$ System of AlO from Combinations of Ultraviolet Transitions

a) Method and data processing

Seven electronic states of the AlO molecule are known through the observation of nine band systems involving either the $X^2\Sigma^+$ ground state or the low-lying $A^2\Pi_i$ state ($T_e \sim 5405.5\text{ cm}^{-1}$). Therefore it appears possible to predict the infrared A–X transition by application of the combination principle in two ways, from the following combinations, $[D^2\Sigma^+ - X^2\Sigma^+] - [D^2\Sigma^+ - A^2\Pi_i]$ or $[C^2\Pi_r - X^2\Sigma^+] - [C^2\Pi_r - A^2\Pi_i]$, hereafter DX–DA or CX–CA. The available analyses of the $D \rightarrow X$ [15] and $D \rightarrow A$ [11] systems restrict the possible predictions to the $A \rightarrow X$ 0–0, 0–1, and 0–2 bands, up to $J \sim 45.5$. We preferred to make use of the $C \rightarrow X$ and $C \rightarrow A$ systems for which more recent analyses [14, 13] permit to predict 6 bands, the 0–0, 0–1 and 0–2 bands up to $J = 64.5$ and the 1–0, 1–1 and 1–2 bands up to $J = 38.5$, without any extrapolation in the branches involving the $A^2\Pi_{1/2}$ sub-state.

Furthermore, it is to be noted that no perturbations have been observed in either the X or the A state with the exception of a weak shift ($\sim 0.1\text{ cm}^{-1}$) of the $A^2\Pi_{3/2}$ ($v = 1, J = 56.5$) level [12].

From the combination CX–CA, 14 different “branches” can be obtained which do not correspond to any of the 12 expected branches of a $^2\Pi \rightarrow ^2\Sigma$ transitions, for example:

$$\begin{aligned} R_2(J)(CX) - R_{21}(J)(CA) &= “Q_{ff}(J)”(AX), \\ {}^S R_{21}(J) - P_{21}(J+2) &= “S_{ee}(J)”, \\ Q_1(J) - P_{12}(J+1) &= “R_{fe}(J)”, \\ {}^O P_{12}(J) - R_{12}(J-2) &= “O_{ff}(J)” \text{ etc.} \dots \end{aligned}$$

These pseudobranches are not observed (the selection rule $+\leftrightarrow +$, $-\leftrightarrow -$ is violated); they are only representative of energy differences between $A^2\Pi_i$ and $X^2\Sigma^+$ levels (in an analogous way the combination DX–DA yields 9 different “branches”). Over 2400 differences could be obtained relative to the six v -connected bands involving the levels $X^2\Sigma^+$ ($v = 0, 1, 2$) and $A^2\Pi_i$ ($v = 0, 1$); they were fitted simultaneously to corresponding calculated term value (X state) or energy matrix eigenvalue (A state) differences using an iterative non-linear least squares procedure. For the X state the usual rotational term-values for $^2\Sigma^+$ states have been used. The energy-matrices used for the description of $^2\Pi$ states have been given elsewhere [16]. The final adjustments are operated after checking the significance of the small parameters within ± 2 standard deviation limits ($2\sigma_p$), removing observed differences deviating by more than 3 times the total standard deviation (3σ) from their calculated values. Thus, a unique and consistent set of rotational constants is derived, generating the remaining 2400 differences with typical rms errors of about 0.06 cm^{-1} .

b) Results: Rovibrational constants for the X and A states

In Table I are gathered the rotational constants for the X and A states which resulted from the final adjustment and corresponding to a total standard deviation $\sigma = 0.053\text{ cm}^{-1}$. In view of obtaining a set of parameters as homogeneous and realistic as possible it appeared preferable to keep a number of them fixed to theoretical or already known values, the adjustment remaining quite equivalent

Table 1. Rotational constants (in cm^{-1}) in the $X^2\Sigma^+$ and $A^2\Pi_i$ states of AlO^a .

| $X^2\Sigma^+$ | $v = 0$ | $v = 1$ | $v = 2$ |
|------------------------|--------------|--------------|--------------|
| T_e | 0 | 965.453(11) | 1916.825(13) |
| B_e | 0.638289(57) | 0.632465(59) | 0.626663(60) |
| $D_e \times 10^5$ | 0.1059(14) | 0.1068(15) | 0.1090(15) |
| $H_e \times 10^{12}$ | −0.574 | −0.581 | −0.589 |
| $\gamma_e \times 10^3$ | 0.73(30) | −0.22(35) | −1.34(37) |

| $A^2\Pi_i$ | $v = 0$ | $v = 1$ |
|----------------------|---------------|--------------|
| T_e | 5281.747(8) | 6002.477(12) |
| B_e | 0.534378(56) | 0.529399(75) |
| $D_e \times 10^5$ | 0.1123(13) | 0.1048(39) |
| $H_e \times 10^{12}$ | −0.239 | −0.243 |
| A_e | −127.6428(97) | −127.926(13) |
| $A_J \times 10^4$ | −0.323(39) | −0.32 |
| $p \times 10^2$ | −0.735(48) | −1.011(52) |
| $p_J \times 10^5$ | −0.271(21) | −0.593 |
| $q \times 10^4$ | 0.37(13) | 0.37 |

^a Numbers in parentheses represent the uncertainty $2\sigma_p$ (twice the standard deviation on the estimated value of the parameter) in unit of the last quoted digit. In the final adjustment some parameters were kept fixed to the values given without indication of $2\sigma_p$ (see text, § 2 b).

as regard to the synthetic spectra. Thus, owing to the strong correlations between H'_v and H''_v constants and the fact that their differences only were revealed at the limit of significance, theoretical values were imposed. To this end, we computed the centrifugal distortion constants for both states, using the method elaborated by Hutson [17] for diatomic molecules and based upon a numerically specified potential curve (RKR potentials were determined for this purpose). The values obtained for H'_v and H''_v are in Table 1; as to the observed D'_v and D''_v values, they show good agreement with the theoretical ones ($D''_0 = 0.110 \times 10^{-5}$; $D'_0 = 0.116 \times 10^{-5} \text{ cm}^{-1}$), indicating that the vibration-rotation approximation is appropriate. In the $A^2\Pi_i$ ($v = 0$) level the parameters A_J , p_J and q appeared significant but in the level $v = 1$ they could not be determined (owing to the lack of available data for high J -values). Consequently, the same values in $v = 1$ as in $v = 0$ were admitted and kept fixed, except for p_J for which the value derived from the analysis of the $E \rightarrow A$ transition [12] was adopted. A difficulty appeared in the determination of the spin-doubling constant γ in the X state. From our adjustments neither the earlier experimental value $\gamma_0 = 0.010 \text{ cm}^{-1}$ [18] nor the more recent ones could be confirmed. Theoretical calculations by Mahieu et al. [19] show that the

spin-doubling in the ground state must be small (arising essentially from second-order interactions with the regular $C^2\Pi$ state) and positive ($\gamma = +0.0035 \text{ cm}^{-1}$) with a very weak vibrational dependence; this result supports the experimental value they found ($\gamma_0 = +0.0050 \text{ cm}^{-1}$) from the analysis of new high-resolution spectra obtained in a low-temperature discharge. Let us also quote the former value $\gamma = +0.0014 \text{ cm}^{-1}$ derived from ESR spectroscopy [8].

When keeping the $\gamma_{0,1,2}$ parameters fixed to the values by Mahieu et al., the quality of our adjustment decreases significantly ($\sigma = 0.071 \text{ cm}^{-1}$). Therefore we finally retained the values reported in Table 1 since they permit to reproduce the observed energy-level differences with the highest accuracy and certainly generate more realistic synthetic spectra.

The molecular constants relative to the equilibrium position in the X and A states are given in Table 2. The values of ω_e and $\omega_e x_e$ in A state which could not be deduced directly from our results were calculated iteratively from Pekeris' formula, assuming that the true potential curve is well represented by a Morse function. They differ significantly from the admitted values $\omega'_e = 728.5 \text{ cm}^{-1}$, $\omega'_e x'_e = 4.15 \text{ cm}^{-1}$ [11]. The same procedure if applied to the ground state yields $\omega''_e = 979.40 \text{ cm}^{-1}$, $\omega''_e x''_e = 6.98 \text{ cm}^{-1}$ in excellent agreement with the observed values.

c) The catalogue

Vacuum line wavenumbers relative to the synthetic spectra of the bands 0–0, 0–1, 0–2, 1–0,

Table 2. Equilibrium constants in cm^{-1} adopted for the $X^2\Sigma^+$ and $A^2\Pi_i$ states of AlO^a .

| Parameter | $X^2\Sigma^+$ | $A^2\Pi_i$ |
|-----------------------|---------------|------------|
| T_e | 0 | 5405.5 |
| ω_e | 979.51 | 731.03 |
| $\omega_e x_e$ | 7.04 | 5.15 |
| B_e | 0.641589 | 0.537261 |
| α_e | 0.005793 | 0.004963 |
| $D_e \times 10^5$ | (0.1098) | (0.1160) |
| $\beta_e \times 10^8$ | (0.91) | (0.74) |
| $H_e \times 10^{12}$ | (−0.57) | (−0.24) |
| $r_e (\text{\AA})$ | 1.6176 | 1.7677 |

^a ω_e and $\omega_e x_e$ in A state have been calculated iteratively from Pekeris' formula. Centrifugal distortion constants obtained from Hutson's method are given in parentheses.

1–1 and 1–2 have been arranged in a catalogue which is available upon request to the authors [20]. They are generated from the set of constants given in Table 1 and listed according to the J -numbering for the eight observable branches, up to $J=65.5$. Let us dwell on the fact that the line wavenumbers calculated beyond $J=21.5$ and $J=38.5$ for the subbands involving the $A^2\Pi_{3/2}$ ($v=1$) and $A^2\Pi_{1/2}$ ($v=1$) levels respectively are extrapolated and should be used cautiously. For comparison, we also give the calculations for (i) the 0–0 band generated from the combination DX–DA, (ii) the 0–0 and 1–0 bands generated from the set of constants obtained when keeping the spin-splitting parameters fixed as discussed above. So, we could verify that the deviations between the corresponding line positions in these different cases were generally small, in any case less than 0.18 cm^{-1} for $J \leq 36.5$.

To sum up, the proposed line positions are expected to represent properly the true spectra at least up to the intensity maxima in the branches which occur for $30.5 \leq J \leq 36.5$ in the range of effective temperatures in the atmospheres of the concerned stars.

3. Aspect of the $A^2\Pi_i \rightarrow X^2\Sigma^+$ Band System

a) Franck-Condon (FC) factors, r -centroids and band intensities

The potential of the A state is shifted to a considerably longer internuclear distance than that of the ground state ($\Delta r_e = 0.150\text{ \AA}$). This leads to a widely opened Condon parabola with overlapping sequences. Using the constants given in Table 2 we have determined the RKR potentials for both states and calculated the FC factors ($q_{v',v''}$) and r -centroids ($r_{v',v''}$) for bands up to $v'=5$ and $v''=8$ (Table 3). These quantities can be useful for evaluating the variation of the electronic transition moment with internuclear separation. The rotational dependence of the FC factors which was found to be negligibly small in all bands, the effect never exceeding 6% of the rotationless factors at $J=60.5$, is not given here. Estimates of relative emission intensities were made following the well-known relation

$$I_{v',v''} = K N_{v'} R_{v',v''}^2 v_{v',v''}^4 q_{v',v''}$$

where K is a constant, $N_{v'}$ the population of the level v' , $R_{v',v''}$ the electronic transition moment at

the value $r_{v',v''}$, and $v_{v',v''}$ the transition frequency. Basing on previous studies [6], the dependence of R_e with $r_{v',v''}$ was taken into account. We have imposed the constraint of a Boltzmann distribution for the upper state population corresponding to a temperature $T=2500\text{ K}$, appropriate to the stars under consideration. A multiplicative factor has been introduced for convenient display, so as the intensity of the strongest 2–0 band is fixed to 100.

b) Aspect of the bands

Twelve rotational branches characterize a $^2\Pi \rightarrow ^2\Sigma$ band. The separation between the $^2\Pi_{1/2}$ and $^2\Pi_{3/2}$ subbands which is large in the A \rightarrow X system ($\sim 128\text{ cm}^{-1}$) shows that the A state closely follows Hund's case (a) coupling. In that case and for an

Table 3. Franck-Condon factors, relative intensities in emission and r -centroids for bands of the A \rightarrow X system of AlO^a.

| v' | v'' | | | | | |
|------|--------------------------|-------------------------|-------------------------|------------------------|------------------------|------------------------|
| | 0 | 1 | 2 | 3 | 4 | 5 |
| 0 | 0.059 42.1 1.6924 | 0.191 56.6 1.7233 | 0.281 28.2 1.7554 | 0.246 6.1 1.7893 | 0.143 0.4 1.8252 | 0.058 0.0 1.8638 |
| 1 | 0.145 78.4 1.6694 | 0.195 49.4 1.6983 | 0.045 4.6 1.7252 | 0.020 0.7 1.7729 | 0.157 1.2 1.8002 | 0.214 0.2 1.8351 |
| 2 | 0.196 100.0 1.6476 | 0.067 17.5 1.6738 | 0.026 3.1 1.7128 | 0.133 6.1 1.7381 | 0.040 0.5 1.7640 | 0.020 0.1 1.8194 |
| 3 | 0.193 88.9 1.6269 | 0.001 0.3 1.6255 | 0.107 13.3 1.6851 | 0.031 1.8 1.7080 | 0.040 0.8 1.7519 | 0.111 0.7 1.7777 |
| 4 | 0.154 61.4 1.6070 | 0.027 6.1 1.6384 | 0.082 10.2 1.6616 | 0.011 0.6 1.7025 | 0.092 2.4 1.7214 | 0.002 0.0 1.7116 |
| 5 | 0.107 35.6 1.5879 | 0.080 16.0 1.6165 | 0.017 1.9 1.6376 | 0.071 4.2 1.6725 | 0.018 0.6 1.6914 | 0.055 0.7 1.7338 |
| 6 | 0.067 18.3 1.5696 | 0.109 18.6 1.5969 | 0.002 0.2 1.6387 | 0.072 0.1 1.6498 | 0.009 0.3 1.6898 | 0.065 1.0 1.7058 |
| 7 | 0.038 8.5 1.5517 | 0.105 15.1 1.5783 | 0.032 2.8 1.6071 | 0.026 1.3 1.6278 | 0.056 1.6 1.6605 | 0.008 0.1 1.6741 |
| 8 | 0.021 3.8 1.5344 | 0.084 10.1 1.5604 | 0.068 5.2 1.5875 | 0.000 0.0 1.5739 | 0.062 1.7 1.6387 | 0.010 0.2 1.6761 |

^a First entry: rotationless FC factor; second entry: relative intensities proportional to $R_{v',v''}^2 \times v_{v',v''}^4 \times q_{v',v''} \times \exp(-G_0(v')/kT)$, for $T=2500\text{ K}$; third entry: rotationless r -centroid (\AA).

inverted ${}^2\Pi$ state, the intensity factors of the different branches are as follows

$$P_2 \text{ and } {}^Q P_{21}: \frac{(2J' + 1)(2J' + 3)}{J' + 1},$$

$$Q_2 \text{ and } {}^R Q_{21}: \frac{(2J' + 1)^3}{J'(J' + 1)},$$

$$R_2 \text{ and } {}^S R_{21}: \frac{4J'^2 - 1}{J' + 1},$$

$$P_1 \text{ and } {}^O P_{12}: \frac{4J'^2 - 1}{J' + 1},$$

$$Q_1 \text{ and } {}^P Q_{12}: \frac{(4J'^2 - 1)(2J' + 3)}{J'(J' + 1)},$$

$$R_1 \text{ and } {}^Q R_{12}: \frac{(2J' + 1)(2J' + 3)}{J'}.$$

Taking account of the coincidence of the satellite branches with main branches due to the very small value of the spin-splitting in the ground state ($R_2(J-1)$ with ${}^R Q_{21}(J)$, etc.) one can expect to observe only four branches in each subband: ${}^S R_{21}$, $R_2 + {}^R Q_{21}$, $Q_2 + {}^Q P_{21}$, P_2 for the ${}^2\Pi_{1/2} \rightarrow {}^2\Sigma^+$ subband with respective intensities in the ratios 1:3:3:1 for the same J'' value (except for the lowest rotational lines) and R_1 , $Q_1 + {}^Q R_{12}$, $P_1 + {}^P Q_{12}$, ${}^O P_{1/2}$ for the ${}^2\Pi_{3/2} \rightarrow {}^2\Sigma^+$ subband with similar intensity ratios.

The bands of the system are degraded to longer wavelengths and four branches show a head reached for very low J -values. For example in the 0–0 band, the heads in the ${}^S R_{21}$ -, R_2 -, R_1 -, and Q_1 -branches are formed at $J = 7.5$, 1.5, 7.5 and 2.5 respectively, far from the intensity maxima in the branches which occur at $J \sim 36.5$ for $T = 2500$ K. The situation is

Table 4. Predicted vacuum line wavenumbers (cm^{-1}) in the 1–0 band of the A \rightarrow X system of AlO.

| J | 1 SR21 | 2 R2 | 3 Q2 | 4 P2 | 5 R1 | 6 Q1 | 7 P1 | 8 OP12 | J |
|------|----------|----------|----------|----------|----------|----------|----------|----------|------|
| 0.5 | 6068.569 | 6067.273 | 6065.694 | | 5939.566 | | | | 0.5 |
| 1.5 | 6069.955 | 6067.374 | 6064.741 | 6063.131 | 5940.926 | 5938.289 | | | 1.5 |
| 2.5 | 6071.128 | 6067.260 | 6063.575 | 6060.891 | 5942.063 | 5938.372 | 5935.736 | 5931.909 | 2.5 |
| 3.5 | 6072.087 | 6066.933 | 6062.195 | 6058.439 | 5942.977 | 5938.233 | 5934.542 | 5929.439 | 3.5 |
| 4.5 | 6072.833 | 6066.393 | 6060.602 | 6055.772 | 5943.670 | 5937.871 | 5933.126 | 5926.747 | 4.5 |
| 5.5 | 6073.365 | 6065.639 | 6058.796 | 6052.893 | 5944.140 | 5937.287 | 5931.488 | 5923.834 | 5.5 |
| 6.5 | 6073.684 | 6064.671 | 6056.777 | 6049.800 | 5944.388 | 5936.481 | 5929.628 | 5920.699 | 6.5 |
| 7.5 | 6073.789 | 6063.490 | 6054.544 | 6046.495 | 5944.414 | 5935.453 | 5927.546 | 5917.342 | 7.5 |
| 8.5 | 6073.680 | 6062.095 | 6052.098 | 6042.975 | 5944.217 | 5934.203 | 5925.242 | 5913.763 | 8.5 |
| 9.5 | 6073.358 | 6060.486 | 6049.440 | 6039.243 | 5943.798 | 5932.730 | 5922.717 | 5909.962 | 9.5 |
| 10.5 | 6072.822 | 6058.664 | 6046.568 | 6035.297 | 5943.157 | 5931.036 | 5919.969 | 5905.940 | 10.5 |
| 11.5 | 6072.073 | 6056.627 | 6043.482 | 6031.139 | 5942.293 | 5929.119 | 5916.999 | 5901.696 | 11.5 |
| 12.5 | 6071.109 | 6054.377 | 6040.184 | 6026.767 | 5941.207 | 5926.980 | 5913.808 | 5897.230 | 12.5 |
| 13.5 | 6069.932 | 6051.913 | 6036.673 | 6022.181 | 5939.898 | 5924.619 | 5910.395 | 5892.543 | 13.5 |
| 14.5 | 6068.541 | 6049.235 | 6032.948 | 6017.383 | 5938.367 | 5922.036 | 5906.760 | 5887.635 | 14.5 |
| 15.5 | 6066.937 | 6046.343 | 6029.010 | 6012.372 | 5936.614 | 5919.231 | 5902.903 | 5882.505 | 15.5 |
| 16.5 | 6065.118 | 6043.237 | 6024.860 | 6007.147 | 5934.638 | 5916.203 | 5898.824 | 5877.154 | 16.5 |
| 17.5 | 6063.085 | 6039.917 | 6020.496 | 6001.709 | 5932.440 | 5912.954 | 5894.524 | 5871.581 | 17.5 |
| 18.5 | 6060.838 | 6036.382 | 6015.919 | 5996.058 | 5930.019 | 5909.482 | 5890.003 | 5865.788 | 18.5 |
| 19.5 | 6058.378 | 6032.634 | 6011.129 | 5990.194 | 5927.376 | 5905.789 | 5885.259 | 5859.773 | 19.5 |
| 20.5 | 6055.703 | 6028.671 | 6006.126 | 5984.116 | 5924.510 | 5901.873 | 5880.295 | 5853.537 | 20.5 |
| 21.5 | 6052.814 | 6024.494 | 6000.910 | 5977.826 | 5921.422 | 5897.736 | 5875.109 | 5847.080 | 21.5 |
| 22.5 | 6049.711 | 6020.102 | 5995.481 | 5971.322 | 5918.112 | 5893.376 | 5869.701 | 5840.403 | 22.5 |
| 23.5 | 6046.393 | 6015.496 | 5989.839 | 5964.605 | 5914.579 | 5888.794 | 5864.072 | 5833.504 | 23.5 |
| 24.5 | 6042.862 | 6010.676 | 5983.984 | 5957.675 | 5910.823 | 5883.991 | 5858.222 | 5826.385 | 24.5 |
| 25.5 | 6039.116 | 6005.641 | 5977.915 | 5950.532 | 5906.845 | 5878.965 | 5852.150 | 5819.045 | 25.5 |
| 26.5 | 6035.155 | 6000.391 | 5971.634 | 5943.176 | 5902.645 | 5873.718 | 5845.858 | 5811.484 | 26.5 |
| 27.5 | 6030.980 | 5994.927 | 5965.140 | 5935.606 | 5898.222 | 5868.249 | 5839.344 | 5803.703 | 27.5 |
| 28.5 | 6026.591 | 5989.248 | 5958.432 | 5927.823 | 5893.577 | 5862.558 | 5832.609 | 5795.701 | 28.5 |
| 29.5 | 6021.987 | 5983.354 | 5951.512 | 5919.827 | 5888.710 | 5856.645 | 5825.653 | 5787.479 | 29.5 |
| 30.5 | 6017.168 | 5977.245 | 5944.378 | 5911.618 | 5883.620 | 5850.511 | 5818.476 | 5779.037 | 30.5 |
| 31.5 | 6012.135 | 5970.922 | 5937.032 | 5903.196 | 5878.308 | 5844.154 | 5811.079 | 5770.374 | 31.5 |
| 32.5 | 6006.887 | 5964.384 | 5929.472 | 5894.560 | 5872.773 | 5837.576 | 5803.460 | 5761.492 | 32.5 |
| 33.5 | 6001.424 | 5957.630 | 5921.699 | 5885.711 | 5867.017 | 5830.777 | 5795.621 | 5752.389 | 33.5 |
| 34.5 | 5995.746 | 5950.662 | 5913.714 | 5876.649 | 5861.037 | 5823.755 | 5787.561 | 5743.066 | 34.5 |
| 35.5 | 5989.854 | 5943.478 | 5905.515 | 5867.373 | 5854.836 | 5816.513 | 5779.280 | 5733.524 | 35.5 |
| 36.5 | 5983.746 | 5936.079 | 5897.103 | 5857.885 | 5848.412 | 5809.048 | 5770.779 | 5723.762 | 36.5 |

not favourable to the observation of characteristic features and the detection of the system in stellar spectra should only be based upon the identification of the rotation lines. The most intense bands of the system appear to be the 2–0, 3–0, 1–0 and 0–1 bands. Among the six calculated bands the 1–0 band is the strongest one and the most favourably situated relatively to the telluric absorption and thus it appears of usefulness to present here the synthetic spectrum of the band (Table 4).

4. Partition Functions and Dissociation Constants

In this section we recompute the internal partition functions for AlO (in the temperature range from 1000 to 8000 K) by taking account of all the observed [21] as well as the unobserved electronic states predicted by Schamps [22] with energies up to $40\,000\text{ cm}^{-1}$; we derive the dissociation constants using for the dissociation energy of AlO the value $D_0^0 = 5.27 \pm 0.04\text{ eV}$ recommended in [21]. A precise knowledge of these quantities is indeed necessary for atmosphere calculations in red giant stars. The most recent works make use of spectroscopic data anterior to the compilation of Huber and Herzberg. Tsuji [23] who gives a polynomial expression for $\log_{10} K_p(T)$ and Scalo and Ross [24] adopt $D_0^0 = 4.60\text{ eV}$ while Johnson and Sauval [25] take $D_0^0 = 5.00\text{ eV}$. Owing to the very important role played by the dissociation energy in the determination of the equilibrium constants, the calculated molecular density strongly depends on the adopted value (at 2500 K, an uncertainty of 0.5 eV in D_0^0 corresponds to a factor of 10 in the molecular density). The value of Huber and Herzberg which is significantly different (in a favourable sense for the production of AlO molecules) is certainly more realistic since it was derived from a critical review of the most recent laser fluorescence studies and a re-interpretation of the long wavelength limit of an absorption continuum. Furthermore, it shows good agreement with the latest mass spectroscopic results ($D_0^0 = 5.24\text{ eV}$ in [26]).

The internal partition functions $Q_{\text{AlO}}(T)$ were obtained by summing the weighted Boltzman factors over the electronic states. For the X and A states (the major contributors in the temperature range considered here) the present data have been used; the large spin-splitting in the A state has been taken into account by separate summation for the

two substates with appropriate electronic statistical weights. For the other observed states, data from [21] were used while for the predicted states the vibrating rotator approximations were assumed.

The values obtained for $Q_{\text{AlO}}(T)$ were then used to determine the equilibrium dissociation constant $K_p(T)$ from the well-known expression [27]

$$K_p(T) = \frac{p_{\text{Al}} p_{\text{O}}}{p_{\text{AlO}}} = \left(\frac{2\pi\mu kT}{h^2} \right)^{3/2} kT \cdot \frac{Q_{\text{Al}}(T) Q_{\text{O}}(T)}{Q_{\text{AlO}}(T)} \exp(-D_0^0/kT)$$

corresponding to the dynamical equilibrium

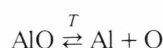


Table 5. Internal partition functions and dissociation equilibrium constants for AlO.

| $T(\text{K})$ | $Q_{\text{AlO}} \times 10^{-4}$ | $\log_{10} K_p$ (dyn · cm ⁻²) |
|---------------|---------------------------------|--|
| 1000 | 0.2921 | −14.9722 |
| 1200 | 0.3861 | −10.4512 |
| 1400 | 0.4961 | −7.2203 |
| 1600 | 0.6244 | −4.7962 |
| 1800 | 0.7738 | −2.9109 |
| 2000 | 0.9474 | −1.4037 |
| 2200 | 1.1482 | −0.1719 |
| 2400 | 1.3793 | 0.8529 |
| 2600 | 1.6435 | 1.7184 |
| 2800 | 1.9438 | 2.4586 |
| 3000 | 2.2828 | 3.0985 |
| 3200 | 2.6632 | 3.6572 |
| 3400 | 3.0874 | 4.1489 |
| 3600 | 3.5580 | 4.5850 |
| 3800 | 4.0774 | 4.9742 |
| 4000 | 4.6483 | 5.3238 |
| 4200 | 5.2730 | 5.6394 |
| 4400 | 5.9543 | 5.9257 |
| 4600 | 6.6948 | 6.1867 |
| 4800 | 7.4974 | 6.4255 |
| 5000 | 8.3652 | 6.6448 |
| 5200 | 9.3011 | 6.8470 |
| 5400 | 10.3085 | 7.0340 |
| 5600 | 11.3907 | 7.2075 |
| 5800 | 12.5514 | 7.3688 |
| 6000 | 13.7941 | 7.5193 |
| 6200 | 15.1228 | 7.6600 |
| 6400 | 16.5414 | 7.7920 |
| 6600 | 18.0540 | 7.9159 |
| 6800 | 19.6648 | 8.0326 |
| 7000 | 21.3780 | 8.1427 |
| 7200 | 23.1981 | 8.2468 |
| 7400 | 25.1294 | 8.3454 |
| 7600 | 27.1764 | 8.4390 |
| 7800 | 29.3437 | 8.5281 |
| 8000 | 31.6359 | 8.6129 |

where the p 's are partial pressures and the Q 's are the internal atomic or molecular partition functions; μ is the reduced mass and D_0^0 the dissociation energy of the molecule. The atomic partition functions for the atoms Al and O were computed using the polynomial coefficients given by Irwin [28].

In Table 5, the internal partition functions and logarithmic dissociation equilibrium constants are listed for the temperature range 1000–8000 K in

steps of 200 K. For practical applications, the tabulated $\log_{10} K_p$ in dyn. cm^{-2} can be approximated as a function of $\theta = 5040.39/T$ by the following polynomial obtained using the least-squares method

$$\log_{10} K_p(\theta) = 11.7987 - 4.9688 \theta - 0.16975 \theta^2 + 0.029733 \theta^3 - 0.0018908 \theta^4,$$

which reproduces the data with a standard-deviation $\sigma = 0.0018$.

- [1] F. E. Baxandall, M.N.R.A.S. **88**, 679 (1928).
- [2] D. N. Davis, *Astrophys. J.* **106**, 28 (1947).
- [3] P. C. Keenan, A. J. Deutsch, and R. F. Garrison, *Astrophys. J.* **158**, 261 (1969).
- [4] R. E. Luck and D. L. Lambert, *Pub. A.S.P.* **86**, 276 (1974).
- [5] P. S. Murty, *Astrophysics and Space Science*, **54**, 509 (1978).
- [6] M. Yoshimine, A. D. McLean, and B. Liu, *J. Chem. Phys.* **58**, 4412 (1973).
- [7] G. Goon and J. R. Auman, *Astrophys. J.* **161**, 533 (1970).
- [8] L. B. Knight and W. Weltner, *J. Chem. Phys.* **55**, 5066 (1971).
- [9] M. J. Sayers and J. L. Gole, *J. Chem. Phys.* **67**, 5442 (1977).
- [10] S. Rosenwaks, R. E. Steele, and H. P. Broida, *J. Chem. Phys.* **63**, 1963 (1975).
- [11] J. K. McDonald and K. K. Innes, *J. Mol. Spectrosc.* **32**, 501 (1969).
- [12] M. Singh and M. D. Saksena, *Can. J. Phys.* **59**, 955 (1981).
- [13] M. Singh and M. D. Saksena, *Can. J. Phys.* **60**, 1730 (1982).
- [14] M. Singh and M. D. Saksena, *Can. J. Phys.* **61**, 1347 (1983).
- [15] M. Singh, *Proc. Ind. Acad. Sci.* **71**, 82 (1970).
- [16] A. Bernard, R. Bacis, and P. Luc, *Astrophys. J.* **227**, 338 (1979).
- [17] J. M. Huston, *J. Phys.* **B14**, 851 (1981).
- [18] A. Lagerqvist, N. E. L. Nilsson, and R. F. Barrow, *Ark. Fys.* **12**, 543 (1957).
- [19] J. M. Mahieu, D. Jacquinet, J. Schamps, and J. A. Hall, *J. Phys.* **B8**, 308 (1975).
- [20] A. Bernard and R. Gravina, *Pub. Obs. Lyon, N°* **15**, 1984.
- [21] K. P. Huber and G. Herzberg, *Molecular Spectra and Molecular Structure IV. Constants of diatomic Molecules*, Van Nostrand-Reinhold, New York (1979).
- [22] J. Schamps, *Chem. Phys.* **2**, 352 (1973).
- [23] T. Tsuji, *Astron. Astrophys.* **23**, 411 (1973).
- [24] J. M. Scalo and J. E. Ross, *Astron. Astrophys.* **48**, 219 (1976).
- [25] H. R. Johnson and A. J. Sauval, *Astron. Astrophys. Suppl. Ser.* **49**, 77 (1982).
- [26] P. Ho and R. P. Burns, *High Temperature Science*, **12**, 31 (1980).
- [27] J. B. Tatum, *Pub. Dom. Astrophys. Obs. Victoria*, **13**, 1 (1966).
- [28] A. W. Irwin, *Astrophys. J. Suppl.* **45**, 621 (1981).